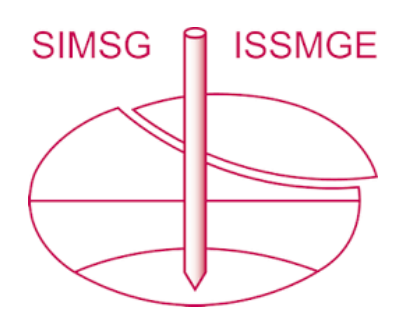
# INTERNATIONAL SOCIETY FOR SOIL MECHANICS AND GEOTECHNICAL ENGINEERING



This paper was downloaded from the Online Library of the International Society for Soil Mechanics and Geotechnical Engineering (ISSMGE). The library is available here:

#### https://www.issmge.org/publications/online-library

This is an open-access database that archives thousands of papers published under the Auspices of the ISSMGE and maintained by the Innovation and Development Committee of ISSMGE.

The paper was published in the Proceedings of the 8<sup>th</sup> International Symposium on Deformation Characteristics of Geomaterials (IS-PORTO 2023) and was edited by António Viana da Fonseca and Cristiana Ferreira. The symposium was held from the 3<sup>rd</sup> to the 6<sup>th</sup> of September 2023 in Porto, Portugal.



## Gradation and state effects on the strength and dilatancy of coarse-grained soils

S. Sharif Ahmed<sup>1</sup>, Alejandro Martinez<sup>1#</sup>, and Jason DeJong<sup>1</sup>

<sup>1</sup> University of California Davis, Department of Civil and Environmental Engineering, Ghausi Hall, Davis CA, USA \*\*Corresponding author: amart@ucdavis.edu

#### **ABSTRACT**

Well-graded soils can be found in nature and in engineered structures, such as dams and embankments. Prediction of their behavior is still an engineering challenge in part due to the lack of data in the literature, arguably due to difficulties associated in testing these soils in the laboratory and *in situ*. Particularly, there is still debate over the effect of the increased range of particle sizes (*i.e.*, widening gradation) on the shear strength and dilatancy of coarse-grained soils. This paper presents the results of drained and undrained isotropically-consolidated triaxial compression tests on six soil mixes of varying gradation. These soils were sourced from a single natural deposit and selectively sieved and mixed to isolate the effects of gradation from those of particle shape and mineralogy. The results indicate that the critical state lines in void ratio – mean effective stress space move downward as the gradation becomes wider. For the same state parameter, the soils with a wider gradation exhibit greater dilatancy and generate negative excess pore pressures with greater magnitudes than the poorly-graded soils. In drained conditions, the greater dilatancy of the well-graded soils leads to greater peak friction angles, while in undrained conditions it leads to greater undrained shear strengths. The results show that these differences in behavior can only be captured when interpreting the results in terms of the state parameter and normalized state parameter, while comparing the results in terms of the void ratio or relative density obscures the effect of differences in gradation.

**Keywords:** Soil gradation; well-graded soils; stress-dilatancy; triaxial testing.

#### 1. Introduction and background

Soils with a wide range of particle sizes are widespread in nature and in engineered structures, such as dams and embankments. Questions remain open regarding the effect of gradation on the mechanical behavior of soils, particularly with respect to the shear strength and dilatancy (e.g., Kokusho and Tanaka 1994). Arguably, this is due to the challenges associated with laboratory testing (i.e., soils with large particles require large specimens) and in-situ testing (i.e., small probe to particle size ratio affects the results). In addition, isolating the effects of gradation from those of particle shape and mineralogy is a pervasive challenge for laboratory investigations.

Dilatancy, the tendency of soils to change volume when they are sheared, results in a coupling between the volume change tendencies and the soil shear strength. The dilatancy of soils depends on the soil properties, such as the particle shape, and the state, typically defined as the combined effects of the effective stress and the void ratio or density. Since the seminal work by Taylor (1948), Rowe (1962) and Bolton (1986), stress-dilatancy frameworks have been developed to provide an elegant and physically-meaningful basis for describing the effects of void ratio and effective stress on the strength of soils. More recent investigations have shed light on the effect of particle shape, soil type, stress history and fabric on the stress-dilatancy relationships (*e.g.*, Vaid and

Sasitharan 1992; Chakraborty and Salgado 2010; Yang and Luo 2015).

Research has also investigated the effects of gradation on the strength and dilatancy of coarse-grained soils. Possibly the most salient effect is that the packing efficiency increases with broadening gradation, meaning that the void ratio at any given effective stress is smaller for well-graded soils (e.g. Youd 1973). Researchers have quantified the effects of the gradation on the critical state line (CSL), small-strain shear modulus, and coordination number of coarse-grained soils (e.g., Menq 2003; Li et al. 2015; Harehdasht et al. 2017; Liu et al. 2021).

Despite advances in the understanding of coarse-grained soil stress-dilatancy and gradation effects, contradicting conclusions have been reported due to the use of different parameters that characterize soil state, including the void ratio (e), relative density ( $D_R$ ), and the difference in void ratio between a given state and the critical state (termed state parameter,  $\xi$ , by Been and Jefferies 1985). This paper provides the results of isotropically-consolidated drained and undrained triaxial tests to examine the role of gradation, quantified by means of the coefficient of uniformity ( $C_U$ ) and the median particle size ( $D_{50}$ ), on the strength and dilatancy of soils considering different state definitions.

#### 2. Materials and methods

#### 2.1. Tested soils

Six coarse-grained soils with different gradations were tested in this investigation. These soils were sourced from the Cape May Formation in New Jersey, USA. The quartz sand- and gravel-sized particles were sieved and mixed to create six soil mixes. This method allowed for isolating the effects of gradation and particle size from those of mineralogy and particle shape.

Three poorly-graded soil mixes, referred to as 100A, 100C, and 100D, were selected to examine the effect of particle size. In addition, three additional mixes referred to as 33ABC, 25ABCD, and 12CU were selected to examine the effect of increasing range of particle sizes. These soil mixes have  $D_{50}$  ranging from 0.18 to 2.58 mm and  $C_U$  from 1.5 to 12.3, as shown in Table 1. A unique aspect of these soil mixes is that since they originate from the same formation, they have negligible differences in their particle roundness and sphericity parameters (Table 1) obtained using the code proposed by Zheng and Hryciw (2015).

Fig. 1a shows the particle size distributions for the six soils. Fig. 1b shows the maximum and minimum void ratios ( $e_{max}$  and  $e_{min}$ ) as a function of  $C_U$ . The results show the expected decrease of  $e_{max}$  and  $e_{min}$  with increasing  $C_U$ , in close agreement the relationship provided by Youd (1973).

**Table 1.** Index properties of tested soils (note: numbers in parentheses correspond to standard deviations).

Soil	D <sub>50</sub> (mm)	Cu	Roundness	Sphericity	Gs
100 A	0.18	1.7	0.39 (0.11)	0.74 (0.13)	2.62
100 C	1.31	1.5	0.42 (0.12)	0.75 (0.12)	2.61
100 D	2.58	1.5	0.45 (0.09)	0.75 (0.12)	2.60
33 ABC	0.51	4.4	0.40 (0.11)	0.75 (0.12)	2.61
25 ABCD	0.80	7.4	0.41 (0.12)	0.75 (0.12)	2.61
12 CU	1.55	12.3	0.46 (0.12)	0.75 (0.12)	2.61

## 2.2. Isotropically-consolidated drained and undrained triaxial compression tests

A triaxial testing system was used to perform all the monotonic drained and undrained triaxial compression experiments. The testing system was equipped with a load cell and an LVDT to measure the axial force and displacement, respectively. The cell and pore pressures were controlled, and the volume changes measured, using two digital pressure volume controllers equipped with pressure sensors. The load and displacement measurements were corrected for piston friction and machine compliance and the volumetric changes were corrected for membrane penetration. However, lubricated end platens were not used.

The specimens had a diameter of 70 mm and a height of about 150 mm, yielding specimen diameter to  $D_{50}$  ratios between 27 and 5.8. All the specimens were

prepared by air pluviation from a constant height. The soil was rained through a series of screens, with different configurations yielding to different densities. According to Sturm (2019) and Humire (2022), this process generates homogenous specimens for these particular soil mixes. After pluviation in the mould, the specimens were stabilized under 10 kPa of vacuum. They were then transported to the triaxial cell. The specimens were then saturated by applying back-pressure to about 400 kPa until a B-value of 0.95 or greater was achieved. After saturation, the specimens were consolidated to the target confining pressure and then sheared at a rate of 10%/hour. The reported relative densities, void ratios, and state parameters correspond to the specimen conditions after isotropic consolidation.

The testing ID is such that "P-x-Q-y" corresponds to soil P at x% relative density at Q drainage condition at an effective stress at consolidation,  $\sigma$ 3c, of y kPa. For example, 100C-40-CD-100 corresponds to soil 100C at 40% relative density tested in drained conditions at  $\sigma$ 3c of 100 kPa.

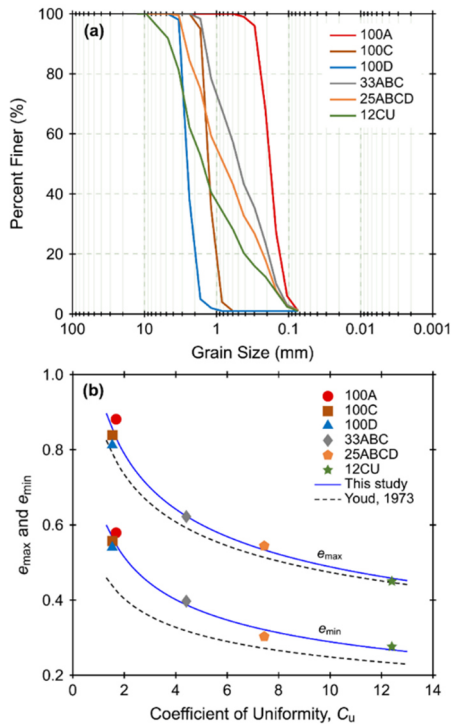


**Figure 1.** (a) Particle size distribution and (b) maximum and minimum void ratios for the tested soils.

#### 3. Results

In total, 69 triaxial compression tests were performed as part of this investigation. The drained and undrained triaxial compression response for the 100C and 12CU soils is described to exemplify the characteristic trends. It is noted that because the CSLs were not known *a priori*, the specimens were prepared at different target  $D_R$ . Further, specimens of different soils having the same  $D_R$  can have different  $\xi$  due to differences in their CSL in relation to their  $e_{max}$  and  $e_{min}$ . This is further discussed in the proceeding sections of the papers.

The results of tests with loose specimens are then used to define CSLs for all six soils. Finally, the results of all tests are analyzed to examine the effect of gradation

and different state definitions on the strength and dilatancy of the soils. The entire dataset is available online in DesignSafe under project PRJ-3719 (Ahmed et al. 2022) and a detailed analysis of the results is provided in Ahmed et al. (2023). This paper provides a summary of the triaxial results and reinterpretation of the critical state data and stress-dilatancy response as a function of different state parameters.

#### 3.1. Drained triaxial compression response

The drained triaxial compression response of the 100C and 12CU soils is typical of coarse-grained soils. Fig. 2 shows the results for specimens of varying density at σ'<sub>3c</sub> of 100 kPa for 100C and 12CU specimens. As shown, as the D<sub>R</sub> is increased, the peak deviator stress (q), initial stiffness and dilative volume changes increase for both soils. The volumetric change response shows a small amount of contraction at small axial strains, followed by significant dilatancy. A unique deviator stress value was not reached at greater axial strains because the dense specimens did not reach the critical state and because they exhibited shear localization. All the specimens followed the characteristic 3:1 stress path in q-mean effective stress (p') space. In e-p' space, all specimens increase in e due to the dilatancy, and the significantly smaller e values for the 12CU soil with a broader gradation are evident.

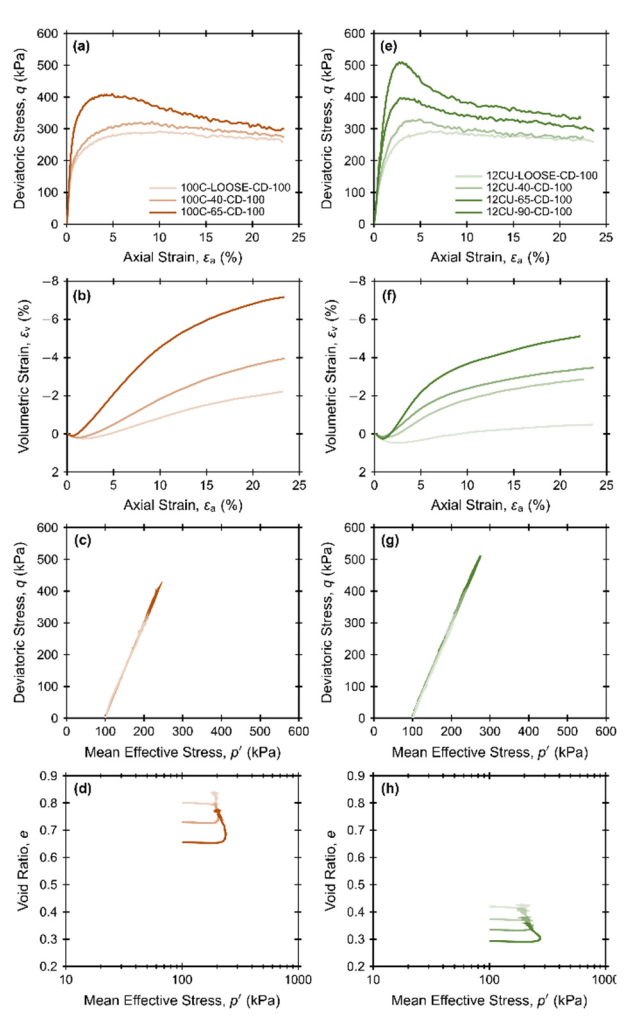


**Figure 2.** Drained triaxial tests on (a)-(d) 100C and (e)-(h) 12CU specimens of varying density (o'<sub>3c</sub> = 100 kPa).

#### 3.2. Undrained triaxial compression response

The undrained triaxial response of 100C and 12CU specimens, shown in Fig. 3, is also typical of coarse-grained soils, with denser soils mobilizing significantly greater deviator stresses due to the generation of negative excess pore pressures ( $\Delta u$ ). At small axial strains, positive  $\Delta u$  with small magnitudes were generated, followed by negative  $\Delta u$  due to the specimen dilatancy. The increase in p' is evident in the stress paths in q-p' and e-p' spaces.

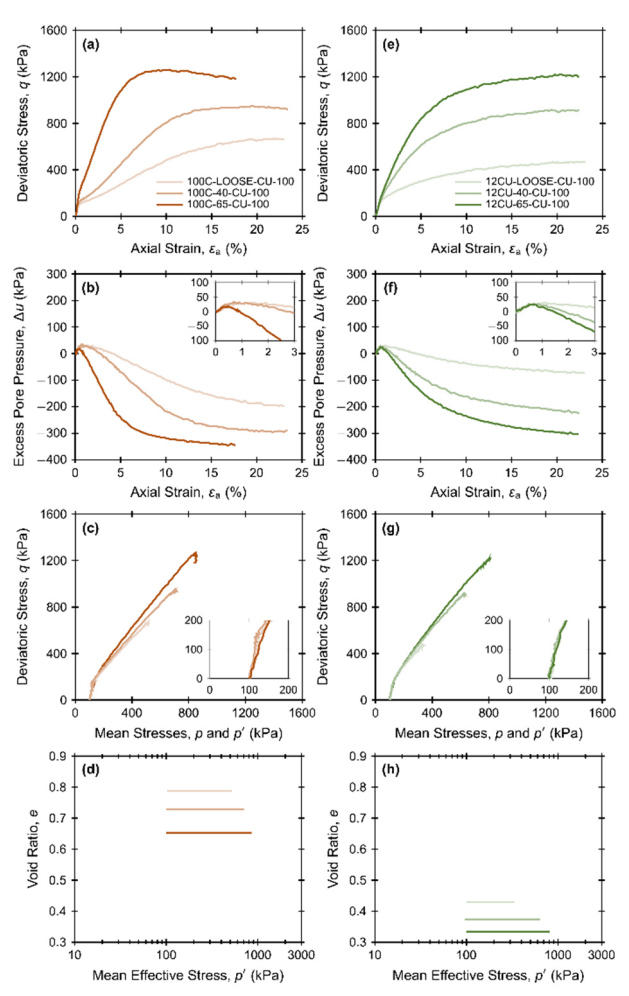


Figure 3. Undrained triaxial tests on (a)-(d) 100C and (e)-(h) 12CU specimens of varying density (σ'3c = 100 kPa).

#### 3.3. Critical state lines

The critical state lines were significantly affected by the differences in gradation, particularly in e-p' space. The CSL lines were determined from the end points of 6 to 8 drained and undrained triaxial tests on loose samples that did not show localization, as shown in Fig. 4a-4f. Ahmed at al. (2023) provides a detailed description of the procedure for selecting the critical state points and Ahmed (2021) provides photographs of the barrelling deformation patterns observed in the specimens. A linear approximation satisfactorily fits the CSLs within the range of tested effective stresses, allowing for a direct comparison of their intercept ( $e_{\Gamma}$ ) and slope ( $\lambda$ ). The CSL shifts downward as the gradation increases due to the increased packing efficiency. This is evidenced by the smallest  $e_{\Gamma}$  value for the 12CU soil (i.e. 0.53), in

comparison to the  $e_\Gamma$  values for the poorly graded soils which are between 1.01 and 1.25. These trends agree with previously published results (Li et al. 2015; Wood and Maeda 2008). While the  $\lambda$  value appears to decrease in magnitude with increasing gradation, from -0.076 for 100A to -0.044 for 12CU, there is a significant effect of the particle size. Namely,  $\lambda$  increases from -0.076 for 100A to -0.161 for 100C to -0.198 for 100D as  $D_{50}$ increases from 0.18 to 1.31 to 2.58 mm, respectively. This increase of  $\lambda$  with particle size reflects an increase in compressibility due to the fact that the force carried by a given particle increases at a faster rate than its stiffness. Namely, Hertz theory indicates that the particle stiffness increases with particle radius with a power of 1/3, while geometrical considerations indicate that the force carried by a particle increase with a power of 2.0.

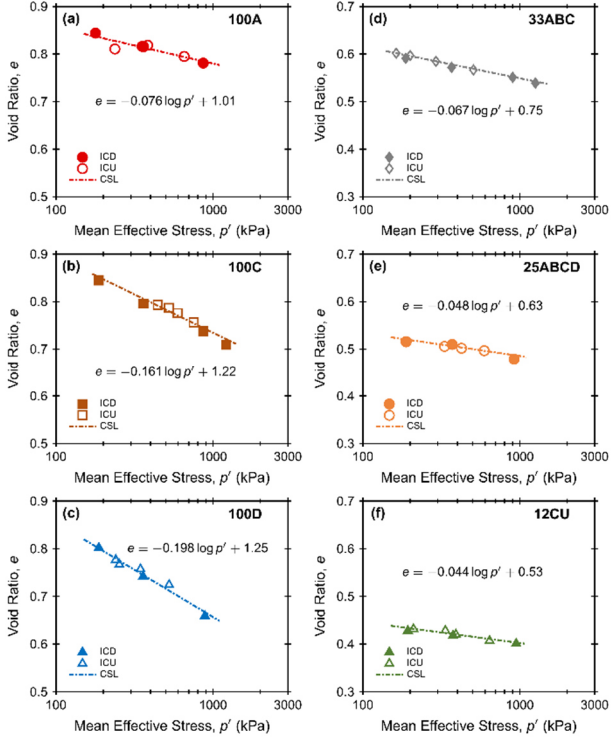


Figure 4. Critical state lines in e-p' space.

The influence of differences in gradation on the slope of the CSL (M) in q-p' space is more modest, as shown in Fig. 5a-5f. Namely, M increased from values between 1.29 and 1.32 for the 100A, 100C and 100D poorly-graded soils, corresponding to critical state friction angles ( $\phi$ '<sub>cs</sub>) from 30.4° to 31.0°, to 1.33 for 33ABC ( $\phi$ '<sub>cs</sub>=31.2°), to 1.36 for 25ABCD ( $\phi$ '<sub>cs</sub>=31.8°), to 1.41 for 12CU ( $\phi$ '<sub>cs</sub>=32.7°). Previous work also reported either modest or negligible effects of gradation on  $\phi$ '<sub>cs</sub> (e.g. Yang and Luo 2017; Harehdasht et al. 2017).

The  $C_U$  and  $D_{50}$  have coupled effects on the CSL parameters. The M parameter increases modestly with increasing  $C_U$ , while it is largely unaffected by changes in  $D_{50}$  (Fig. 6a and 6d). The  $e_\Gamma$  parameter is influenced by both  $C_U$  and  $D_{50}$ . Namely, it decreases sharply as  $C_U$  is increased, and it increases modestly as  $D_{50}$  is increased (Fig. 6b and 6e). While the slope of the CSL decreases as  $C_U$  is increased, the increase due to increases in  $D_{50}$  is greater (Fig. 6c and 6f). It is thus important to consider

the effects of both gradation and particle size in CSL parameters, especially in the e-p' plane.

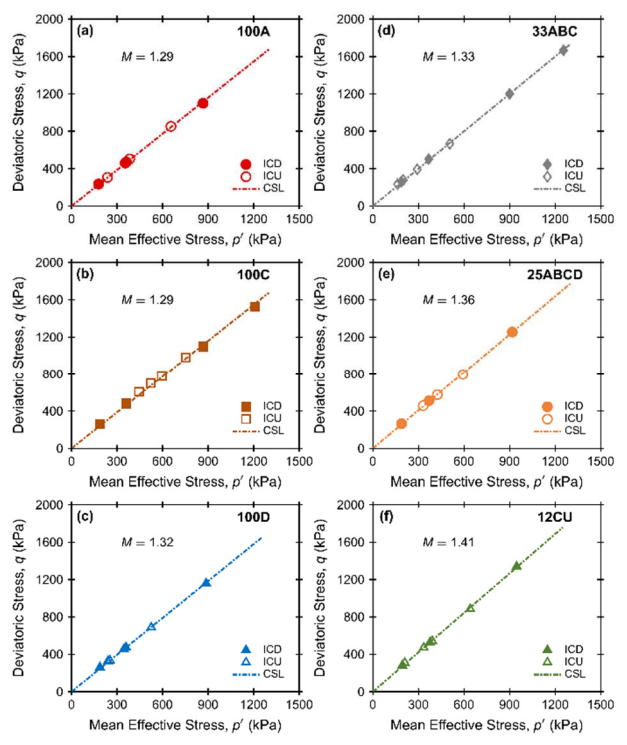
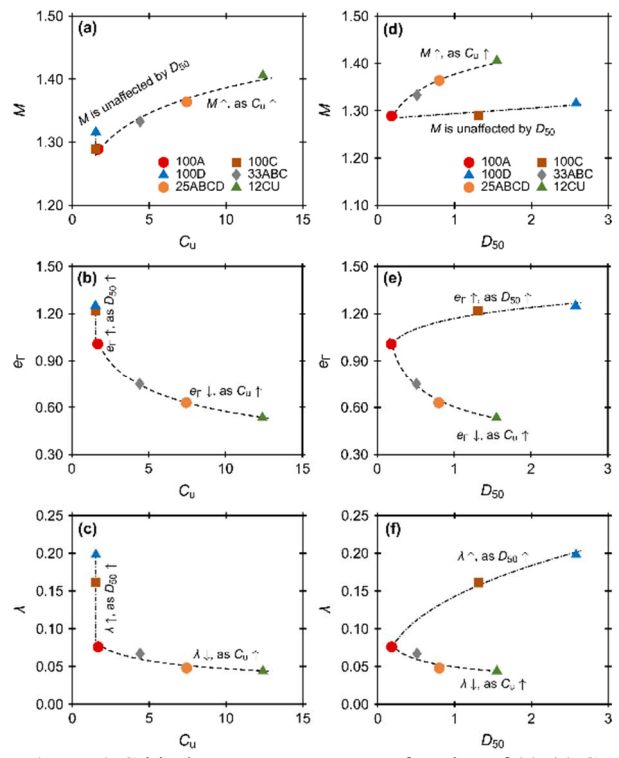


Figure 5. Critical state lines in q-p' space.



**Figure 6.** Critical state parameters as a function of (a)-(c) C<sub>U</sub> and (d)-(f) D<sub>50</sub>.

### 3.4. Trends in stress-dilatancy as a function of various state parameters

While all the soils exhibited potential to dilate in drained conditions (Fig. 2) and develop negative  $\Delta u$  in undrained conditions (Fig. 3), trends regarding the effect

of gradation on the stress-dilatancy are expected to be more robust within the critical state framework.

The effect of gradation can be examined by comparing results for similar initial state parameters, as shown in Fig. 7a-7h for specimens with  $\xi$  of -0.14 to -0.17. In drained conditions, the peak q and maximum rate of dilatancy are greater for the more broadly graded soils (i.e. 12CU, 25ABCD), while the poorly-graded soils with larger particle sizes (i.e. 100C, 100D) show the smallest q and rate of dilatancy. The stress paths show the smaller e and greater p' increases for soils with greater  $C_U$ .

The more widely graded soils mobilized greater deviator stresses due to the generation of negative  $\Delta u$  with greater magnitude (Fig. 7e-7h). This is particularly clear when comparing the response of the 12CU and 25ABCD specimens with the 100C and 100D specimens, while the 100A specimen generated similar  $\Delta u$  magnitudes as the 12CU specimen. The stress paths clearly show the dilatancy-induced increases in p'.

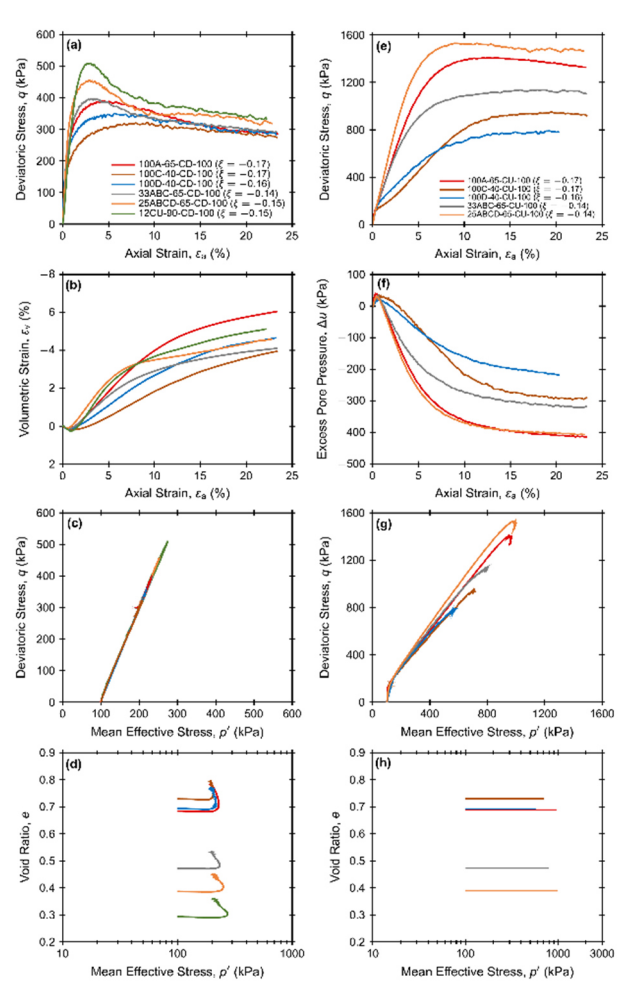


**Figure 7.** Comparison of (a)-(d) drained and (e)-(h) undrained triaxial compression response for dense specimens with similar initial state parameters.

Relevant parameters from the tests, including the peak friction angle  $(\phi'_p)$ , maximum dilatancy angle  $(\psi)$ , and greatest magnitude of negative excess pore pressures  $(\Delta u_{min})$ , can be extracted and plotted in terms of different parameters that describe state. These include the state parameter, relative density, void ratio, and normalized state parameter  $(\xi/\xi_1)$ . The  $\xi/\xi_1$  parameter is defined as the state parameter normalized by the difference between

 $e_{max}$  and  $e_{min}$  (Konrad 1988). The results show the expected trends of increases in  $\phi$ '<sub>p</sub>,  $\psi$  and  $\Delta u_{min}$  as  $\xi$ ,  $\xi/\xi_1$  and e decrease and as  $D_R$  increases.

For any given  $\xi$ , the drained tests show an increase in mobilized  $\phi$ '<sub>p</sub> as the gradation becomes wider (Fig. 8a). These results go in hand with the trends in  $\psi$ , showing increasing values for any  $\xi$  as the gradation becomes wider (Fig. 9a). These results help explain the  $\Delta u_{min}$  from undrained tests, showing greater magnitudes as  $C_U$  is increased due to the increase in dilative behavior (Fig. 10a). The results also show particle size effects, with the finer poorly-graded soil 100A mobilizing greater  $\phi$ '<sub>p</sub>,  $\psi$  and  $\Delta u_{min}$  for any given  $\xi$  than the coarser 100C and 100D soils. The results show similar trends when plotted in terms of  $\xi/\xi_1$ , with the exception that the  $\phi$ '<sub>p</sub>,  $\psi$  and  $\Delta u_{min}$  values for 100A are shifted rightward, thus plotting close to the more well-graded 25ABCD and 12CU soils (Figs. 8b, 9b and 10b).

The trends in  $\phi^{\prime}_{p}$ ,  $\psi$  and  $\Delta u_{min}$  versus void ratio are reasonably fitted with linear functions (Figs. 8c, 9c and 10c); however, the plots clearly show that gradation affects the possible range of void ratios that can be attained by the soils. In fact, the results show no common e values between the poorly-graded soils and the three more broadly graded soils, highlighting that the use of a common void ratio as the basis of comparison for soils of different gradation greatly biases the results. When examined in terms of  $D_R$ , the trends are unclear (Figs. 8d, 9d and 10d). Little systematic differences between the soils is observed apart from the 25ABCD soil mobilizing greater  $\phi^{\prime}_{p}$  and  $\psi$ . Additionally, the results show significant scatter at  $D_R$  values smaller than 40%.

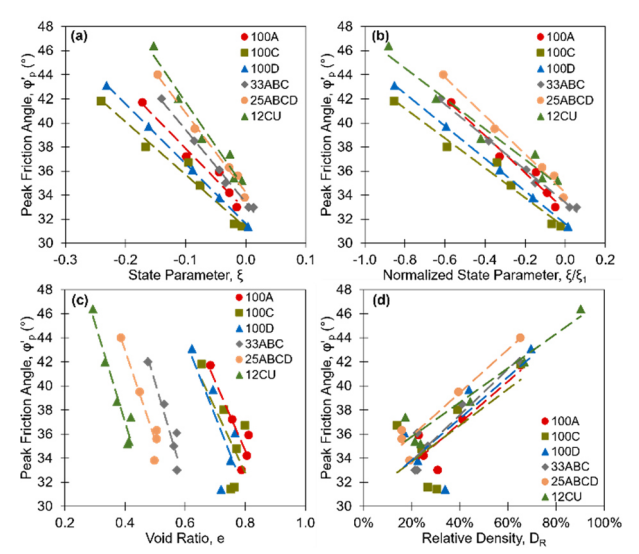


**Figure 8.** Peak friction angle as a function of (a) state parameter, (b) normalized state parameter, (c) void ratio and (d) relative density.

The scatter in the  $\phi^{\prime}_{p}$ ,  $\psi$  and  $\Delta u_{min}$  results when analysed in terms of  $D_{R}$  are due to the effects of gradation and particle size on the difference between the initial state and the critical state. In other words, a common  $D_{R}$  value does not correspond to a common state parameter. Fig. 11 shows relative density at critical state ( $D_{R,CS}$ ) values as a function of  $C_{U}$  and  $D_{R}$  for  $p^{\prime}$  of 500 and 1000 kPa. The  $D_{R,CS}$  values for each soil were calculated from their

corresponding CSL lines. The results show that increases in  $C_U$  cause a decrease in  $D_{R,CS}$  (i.e. from 33% to 24% for p'=1000 kPa). Also, for similar  $C_U$ , increases in  $D_{50}$  cause an increase in  $D_{R,CS}$  (i.e. from 33% to 57% for p'=1000 kPa).

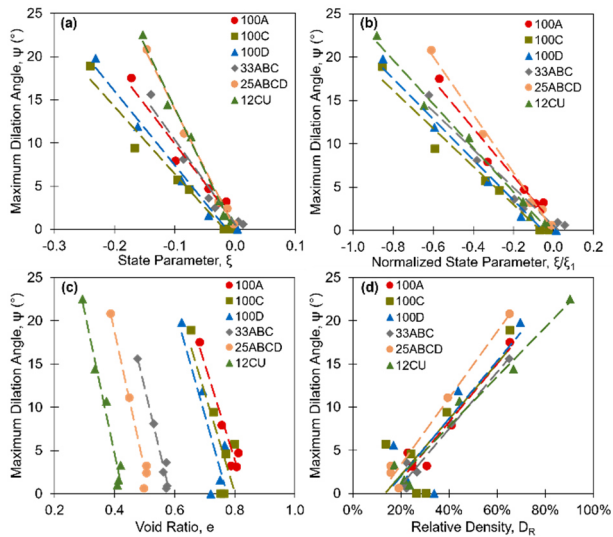


**Figure 9.** Maximum dilatancy angle as a function of (a) state parameter, (b) normalized state parameter, (c) void ratio and (d) relative density.

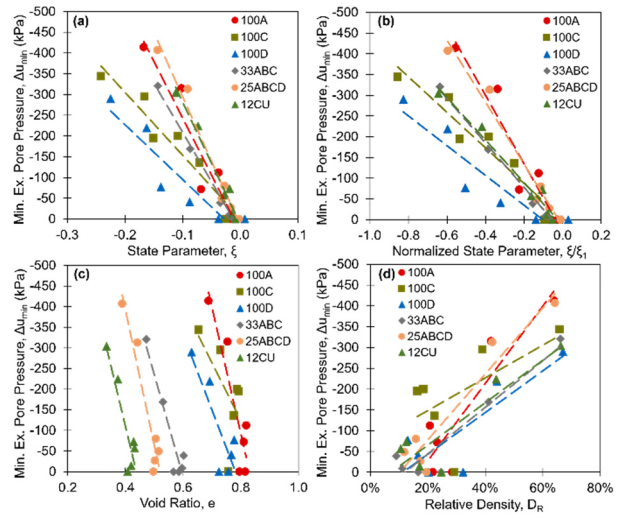


**Figure 10.** Minimum excess pore pressure as a function of (a) state parameter, (b) normalized state parameter (c) void ratio, and (d) relative density.

#### 4. Conclusions

This paper presents the results of a series of isotropically-consolidated drained and undrained triaxial compression tests on soil specimens with systematic differences in gradation. The six tested soils were sourced from the same formation by mechanically sieving and remixing, thus isolating the effects of gradation and particle size from those of other parameters such as particle shape and mineralogy.

The triaxial compression response of all six soils shows the expected trends, with denser specimens dilating more in drained conditions and generating greater magnitudes of negative excess pore pressured in undrained conditions. Drained and undrained tests on loose specimens at different confining pressures were used to estimate the critical state lines of the soils. The results indicate a modest increase in the slope of the CSL in q-p' space, and a sharp decrease in the intercept and a small decrease in the slope of the CSL in e-p' space, as the gradation is broadened. The slope of the CSL in q-p' space was unaffected by the particle size, while both the intercept and slope of the CSL in e-p' space increased with increasing particle size. The results of all the triaxial tests are available online (Ahmed et al. 2022).

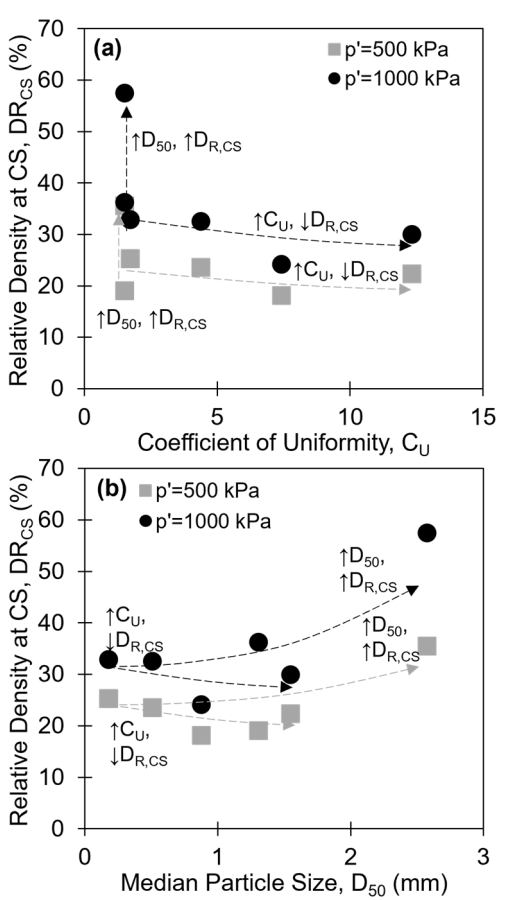


**Figure 11.** Relative density at critical state as a function of (a)  $C_U$  and (b)  $D_{50}$ .

The state parameter and normalized state parameter produced more robust relationships between triaxial response parameters characterizing the stress-dilatancy of the materials (i.e. peak friction angle, maximum dilatancy angle, and greatest magnitude of negative excess pore pressures) and soil gradation. Specifically, for any given state parameter or normalized state parameter, the soils with a broader gradation mobilized greater peak friction angles, maximum dilatancy angles and generated greatest magnitudes of negative excess pore pressures. Comparing the results in terms of a common void ratio value is impossible because of the lack of common void ratio values that can be attained by the poorly-graded and well-graded soils. While the peak friction angle, maximum dilatancy angle, and greatest magnitude of negative excess pore pressures increased with increasing relative density, the relative density obscured the effects of gradation and particle size. This is because the relative density at critical state is shown to decrease with broadening gradation and increase with increasing particle size.

#### **Acknowledgements**

The National Science Foundation (NSF) provided the funding for this work under grant No. CMMI-1916152 and also funded the Natural Hazards Engineering Research Infrastructure (NHERI) shared use centrifuge facility at the University of California at Davis under grant No. CMMI-1520581. The authors would also like to thank Katerina Ziotopoulou, Rachel Reardon, Francisco Humire, Mandeep Singh Basson, Nathan Love, Trevor Carey, and Anna Chiaradonna for their insights and recommendations.

#### References

- Ahmed, S.S. 2021. "Study on particle shape, size and gradation effects on the mechanical behavior of coarse-grained soils." Ph.D. dissertation, University of California, Davis.
- Ahmed, S. Martinez, A. DeJong, J. 2022. "Isotropically-consolidated drained and undrained triaxial compression tests on soils of varying gradation", in In Situ Characterization of Well-graded Coarse-grained Soils: Monotonic Triaxial Tests on Soils of Varying Gradation. DesignSafe-CI. <a href="https://doi.org/10.17603/ds2-crtg-j217">https://doi.org/10.17603/ds2-crtg-j217</a>
- Ahmed, S., Martinez, A., and DeJong, J.T. 2023. "Effect of Gradation on the Strength and Stress-Dilation Behavior of Coarse-Grained Soils in Drained and Undrained Triaxial Compression." J. Geotech. Geoenv. Eng. 149, no. 5.
- Been, K, and Jefferies, M. G. 1985. "A state parameter for sands." Géotechnique 35, no. 1: 99–112.
- Bolton, M. D. 1986. "The strength and dilatancy of sands." Géotechnique 36, no.1: 65–78.
- Chakraborty, T., and Salgado, R. 2010. "Dilatancy and shear strength of sand at low confining pressures." J. Geotech. Geoenviron. Eng., 136, no. 3: 527–532.
- Humire, F. 2022. "Liquefaction and Post-Liquefaction Behavior of Coarse-Grained Soils." Ph.D. dissertation, University of California, Davis.
- Harehdasht, S. A., Karray, M., Hussien, M. N. and Chekired, M. 2017. "Influence of particle size and gradation on the stress-dilatancy behavior of granular materials during drained triaxial compression." Int. J. Geomech., 17, no. 9.
- Kokusho, T., and Tanaka, Y. 1994. "Dynamic Properties of Gravel Layers Investigated by In-Situ Freezeing

- Sampling." Ground Failures Under Seismic Conditions, ASCE Geotechnical Special Publication, 44: 121–140.
- Konrad, J.M. 1988. "Interpretation of flat plate dilatometer tests in sands in terms of the state parameter." Géotechnique, 38, no. 2: 263-277.
- Li, G., Liu, Y. J., Dano, C. and Hicher, P. Y. 2015. "Grading-dependent behavior of granular materials: from discrete to continuous modeling." J. Eng. Mech. 141, no. 6.
- Liu, D., O'Sullivan, C., and Carraro, J. A. H. 2021. "Influence of Particle Size Distribution on the Proportion of Stress-Transmitting Particles and Implications for Measures of Soil State." J. Geotech. Geoenviron. Eng. 147, no. 3.
- Menq, F.-Y. 2003. "Dynamic properties of sandy and gravelly soils." Ph.D. dissertation, University of Texas Austin.
- Rowe, P. W. 1962. "The stress-dilatancy relation for static equilibrium of an assembly of particles in contact." Proceedings of the Royal Society of London. Series A. Mathematical and Physical Sciences, 269, no. 1339: 500–527.
- Sturm, A. P. 2019. "On the liquefaction potential of gravelly soils: Characterization, triggering and performance." Ph.D. dissertation, University of California, Davis.
- Taylor, D. W. 1948. Fund. Soil Mech. John Wiley & Sons, New York, NY.
- Vaid, Y. P., and Sasitharan, S. 1992. "The strength and dilatancy of sand." Can. Geotech. J. 29, no. 3: 522–526.
- Wood, D. M., and Maeda, K. 2008. "Changing grading of soil: effect on critical states." Acta Geotechnica 3: 3–14.
- Yang, J., and Luo, X.D. 2015. "Exploring the relationship between critical state and particle shape for granular materials." J. Mech. Phys. Sol., 84 (November): 196-213.
- Yang, J., and Luo, X. D. 2017. "The critical state friction angle of granular materials: does it depend on grading?" Acta Geotechnica. 13, no. 3: 535–547.
- Youd, T. L. 1973. "Factors controlling maximum and minimum densities of sands. Evaluation of Relative Density and its Role in Geotechnical Projects Involving Cohesionless Soils." In STP 523. ASTM International. West Conshohocken, PA. 98–112.
- Zheng, J., and. Hryciw. R. D. 2015. "Traditional soil particle sphericity, roundness and surface roughness by computational geometry." Géotechnique 65, no. 6: 494– 506